Use of three-dimensional–printed custom-made prosthesis to treat unicondylar femoral defect secondary to pathological fracture caused by giant cell tumor

Yuqing Ji ⑩**, Yuxian Wu and Jianmin Li**

Abstract

Objective: To evaluate the short-term effectiveness of using a three-dimensional (3D)-printed custom-made prosthesis to repair unicondylar femoral defects.

Methods: We retrospectively reviewed 26 patients with a primary pathological fracture of the distal femur caused by a giant cell tumor. All patients had unicondylar defects involving the articular surface. Twelve patients were treated with a 3D-printed custom-made prosthesis to repair the unicondylar defect (3D-printed group). The other 14 patients were treated with total knee replacement (TKR group). The operation time, blood loss, Musculoskeletal Tumor Society score, range of motion, local recurrence, and complications were statistically compared.

Results: The operation time was significantly shorter and the blood loss was significantly less in the 3D-printed group than in the TKR group. The Musculoskeletal Tumor Society scores were significantly higher in the 3D-printed group than in the TKR group from 3 to 24 months postoperatively. The range of motion was significantly better in the 3D-printed group than in the TKR group at 6 and 9 months postoperatively.

Conclusions: 3D-printed custom-made prostheses provide better short-term functional results than does TKR.

Department of Orthopaedic Oncology, Qilu Hospital (Qingdao), Cheeloo College of Medicine, Shandong University, Qingdao, Shandong, China

Corresponding author:
Jianmin Li, Department of Orthopaedic Oncology, Qilu Hospital (Qingdao), Cheeloo College of Medicine, Shandong University, 758 Hefei Road, Qingdao, Shandong 266035, China.
Email: bonetumor_ljm@163.com

Introduction

Giant cell tumors (GCTs) of the bone account for approximately 5% of all primary bone tumors.[1] The rate of pathological fracture at presentation in these patients ranges from 4% to 50%,[2] with 12% of the fractures located at the distal end of the femur.[2] Pathological fracture associated with a distal femoral GCT frequently leads to joint surface defects, which are difficult to repair. Such joint destruction is often confined to one condyle because of the eccentric growth of the GCT;[3] however, conventional methods require the removal of both condyles together following total knee replacement (TKR), leading to a low prosthesis survival rate and the need for multiple joint replacement,[4–6] especially in relatively young patients. Considering that these lesions destroy part of the articular surface, partial repair of the articular surface is reasonable.

With the technological developments in recent decades, three-dimensional (3D) printing technology has reportedly enhanced the accuracy and individualization of orthopedic surgeries.[7–9] The use of 3D printing technology in orthopedic surgery allows a greater freedom of prosthetic design and the fabrication of more complex shapes.[10] Thus, it is possible to reconstruct defects in musculoskeletal oncology with personalized custom-made prostheses.[11] This technology can increase the accuracy of the reconstruction and reduce the rate of postoperative complications, thereby potentially improving stability.[12]

The use of 3D printing technology to repair unicondylar defects caused by pathological fractures has not been reported to date, and a comparative analysis of this approach versus traditional TKR has not been conducted. We performed a retrospective study to (1) evaluate the feasibility of 3D-printed custom-made prosthesis in repairing unicondylar defects caused by pathological fractures induced by GCTs of the distal femur and (2) determine the functional results, complications, and outcomes during short-term follow-up.

Methods

Patients

The inclusion criteria for the operation were a histologically confirmed GCT of the distal femur; a defect of the distal articular surface of one side of the femoral condyle caused by pathological fracture; and a follow-up time of >24 months, after which the follow-up data were complete. The exclusion criteria were nonsurgical treatment; combination with cruciate ligament, meniscus, or collateral ligament injury or serious joint degeneration; bilateral condylar lesions or multiple articular surface defects; and preoperative treatment with denosumab. We retrospectively analyzed our database and identified 26 patients with a unicondylar defect caused by pathological fracture secondary to a GCT of the distal femur treated from January 2012 to January 2018.

The following data were collected: age, sex, lesion site, Campanacci classification,[13] operation time, blood loss, Musculoskeletal Tumor Society (MSTS) scores,[14] local recurrence, and complications. Blood loss was defined as the amount of bleeding during the operation. The operation time was defined as the duration of time from the beginning of skin incision to closing of the incision. The MSTS scoring system includes six measures: pain, function, emotional acceptance, and three specific factors for evaluating the upper or lower limb. For each of the six measures, values of 0 to 5 are assigned with a total maximum score of 30.[14] According to the surgical intervention performed, the patients were divided into those who underwent treatment with a 3D-printed custom-made prosthesis (3D-printed group) and those who underwent TKR (TKR group). All surgeries were performed by the same medical team. The reporting of this study conforms to the STROBE statement.[15] This study was approved by the by the Ethics Committee of Qilu Hospital of Shandong University Medical Ethics Committee (approval no. 2015087). All patients gave written informed consent to be included in this study upon their admission to the hospital.

Design and manufacturing of 3D-printed custom-made prosthesis

All the patients were evaluated by preoperative imaging as shown in Figure 1(a)–(d). The preoperative plain radiography and magnetic resonance imaging findings of tumor-induced erosion of the distal femur were evaluated. The distal femurs on both the affected side and healthy side were scanned with computed tomography at 1-mm slice intervals. The Digital Imaging and Communications in Medicine format data of the computed tomography images were then transferred to Mimics Medical 21.0 software (Materialise NV, Leuven, Belgium). Masks of both distal femurs were established using the Region Growing command. 3D models of both distal femurs were obtained using the Calculate Part command. 3D models of the distal femurs of the affected side before being eroded by the tumor were established using the mirror command from the healthy side. Boolean logic was then used to model the defect-containing articular surface from the models before and after pathological fracture. Geomagic Studio 12 (3D Systems, Rock Hill, SC, USA) was used to help transform the defective articular surface model into a solid model, which was edited using Siemens NX 12.0 software (Siemens Digital Industries Software, Plano, TX, USA).

Siemens NX 12.0 software was used to make the defect-containing articular surface 0.5 mm lower than the articular surface of the normal knee, which was measured by magnetic resonance imaging. To increase the stability of the defect-containing articular surface, screws that pass through the defect-containing articular surface of the prosthesis and an extra plate for fixation of the prosthesis were designed together with engineers using Siemens NX 12.0 software (Figure 2). A model of the lesion was printed and used to elucidate the condition in more detail before surgery (Figure 3(a), (b)). The final prosthesis was then printed with the electron beam melting technology of titanium powder, and the articular surface was highly polished (Figure 3(c), (d)). The design and manufacture of each personalized 3D-printed prosthesis (Shanghai Shengshi Co., Shanghai, China) took approximately 2 weeks.

Surgical procedure

3D-printed group: The surgery was performed under general anesthesia. The tumor was removed by curettage, which was performed through the window of the
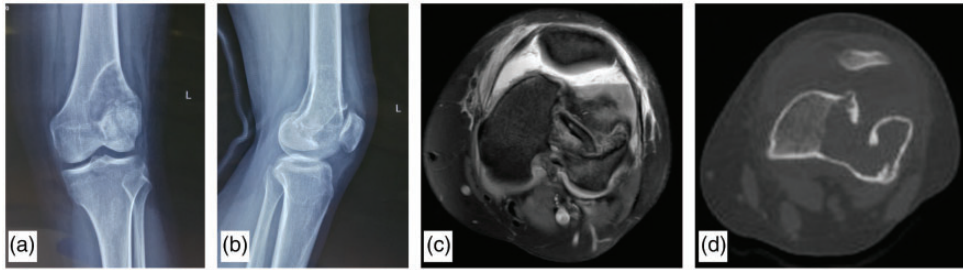
Figure 1. Imaging examinations of a woman aged 29 years in the 3D-printed group. (a) and (b) The preoperative radiographs show a pathological fracture secondary to a giant cell tumor in the left distal femur. The (c) magnetic resonance imaging scans and (d) computed tomography scans show an articular surface defect caused by the pathological fracture.
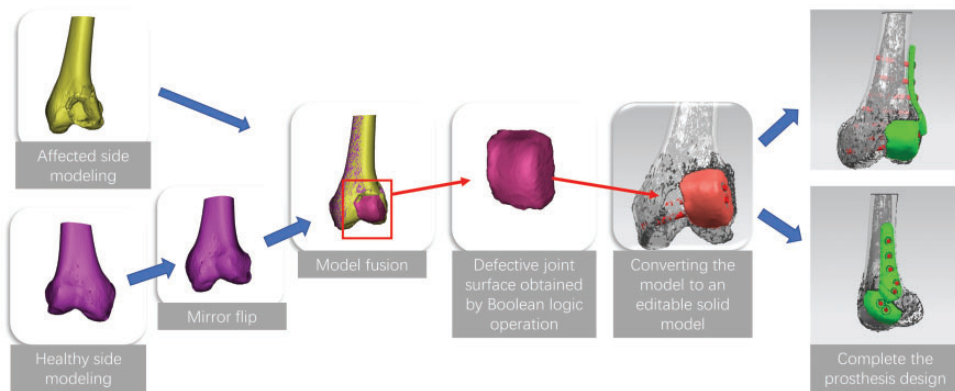

Figure 2. Flow chart of the design of the 3D-printed custom-made prosthesis to repair the articular surface defect.

defect-containing part of the articular surface. If the window of the defect-containing part was not large enough to scrape away all the tumor tissues, then an additional window was opened at the distal femur not covered by the articular surface. After removing all visible tumor tissues, the tumor cavity was cauterized with an electric knife and expanded with a high-speed burr (Figure 3(e)). After the curettage was completed, anhydrous alcohol and distilled water pulse irrigation were used to rinse the cavity. The tumor cavity was then filled with bone cement. The 3D-printed prosthesis was installed

before the setting of the bone cement. The installation process ensured that the joint surfaces were in the proper position (Figure 3(f)–(h)).

TKR group: The surgery was performed under general anesthesia. A median incision was performed in front of the knee joint, and the distal femur was exposed outside the diseased bone or tumor mass. Osteotomy of the distal femur was performed according to the preoperative measurements. Tibial osteotomy was performed in the same manner as a standard knee arthroplasty. A tumor-type prosthesis (Beijing Chunli Co., Beijing, China) was
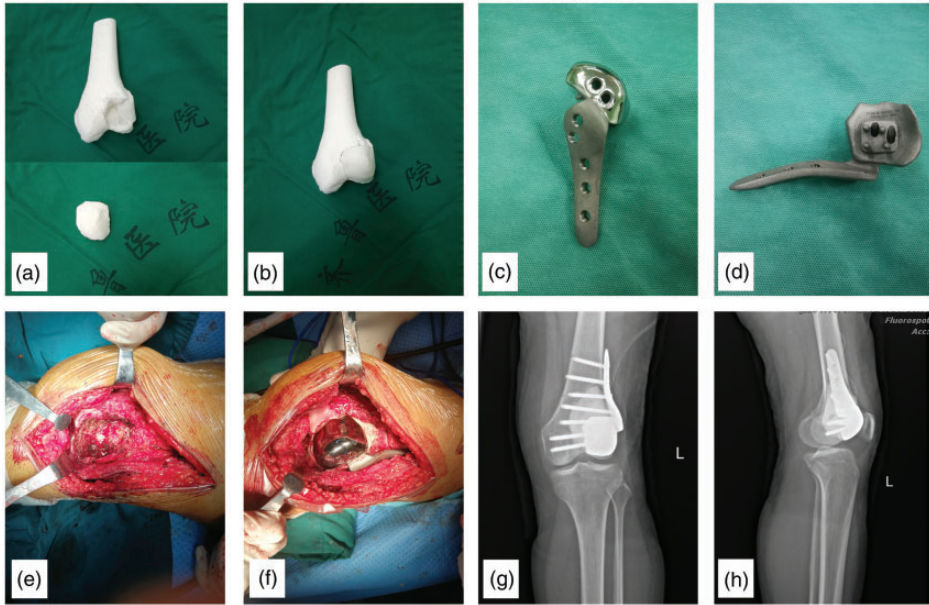
Figure 3. The 3D-printed prosthesis and surgical procedures. (a) 3D-printed models of the distal femur containing a defect of the articular surface caused by a pathological fracture secondary to a giant cell tumor. (b) The defect of the articular surface. (c) and (d) The 3D printed prosthesis. (e) Intraoperative pictures show that the tumor tissue has been scraped off. (f) The distal femur showing that the defect of the articular surface has been restored by the 3D-printed prosthesis and that the prosthesis has been installed and fixed. (g) and (h) Postoperative radiographs of the distal femur.
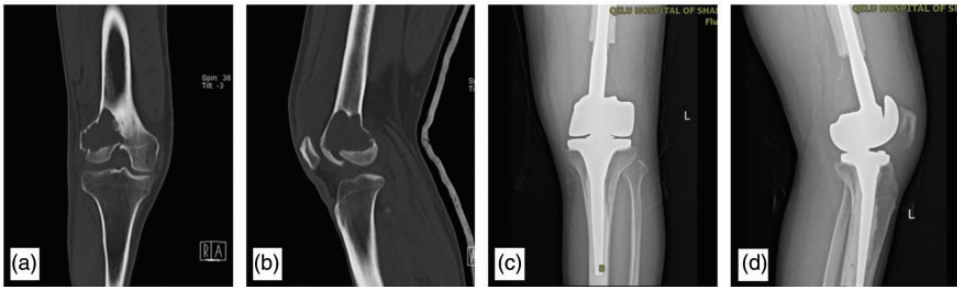

Figure 4. Preoperative and postoperative imaging examinations of a 54-year-old man in the TKR group. (a) and (b) The preoperative computed tomography images show a pathological fracture secondary to a giant cell tumor in the left distal femur. (c) and (d) Radiographs after TKR of the left knee.

reconstructed by conventional methods after tumor resection (Figure 4(a)–(d)).

Postoperative management

The postoperative management of the two groups was similar. Range of motion (ROM) exercises of the knee were performed from postoperative day 1. The patient was allowed non-weight-bearing standing and walking at 7 days after surgery. Partial weight-bearing with crutches was encouraged starting from the second week after surgery, followed by gradual

conversion to full weight-bearing. The patient was followed up every month for the first 3 months and then every 3 months thereafter. The oncology outcomes and radiographic findings were assessed at each follow-up.

Statistical analysis

Continuous data are expressed as mean ± standard deviation. The independent-samples t test was used to compare the age, operation time, bleeding volume, ROM, and MSTS score between the two groups. The χ^2 test was used to analyze the sex, tumor location, postoperative complications, and recurrence rate in the two groups. A p-value of <0.05 was considered statistically significant. The statistical analysis was performed using IBM SPSS Statistics for Windows, Version 22.0 (IBM Corp., Armonk, NY, USA).

Results

Operational outcomes

Twenty-eight patients meet the inclusion criteria from January 2012 to January 2018. Two patients treated with TKR were excluded because of preoperative use of denosumab, and 26 patients were finally involved in this study. Twelve patients were treated with 3D-printed custom-made prostheses (3D-printed group), comprising seven men and five women with a mean age of 42.2 years (range, 29–69 years). Fourteen patients were treated with TKR (TKR group), comprising nine men and five women with a mean age of 45.4 years (range, 34–68 years). The patients' main characteristics are shown in Tables 1 and 2. All operations were performed successfully, and no intraoperative complications occurred. The mean operating time in the 3D-printed group was 123.3 ± 20.7 minutes (interquartile range (IQR), 100–160

minutes), which was significantly lower than that in the TKR group (146.4 ± 18.8 minutes; IQR, 120–170 minutes) (p = 0.006). The mean blood loss during the operation in the 3D-printed group was 109.6 ± 15.7 mL (IQR, 90–140 mL), which was significantly lower than that in the TKR group (182.1 ± 31.9 minutes; IQR, 130–225 minutes) (p < 0.001).

Oncological outcomes

The mean follow-up period was 33.5 months (range, 26–43 months). One female patient in the TKR group developed recurrence 9 months postoperatively, and she underwent a second resection. All the other patients remained disease-free during the follow-up period.

Postoperative functional status

The recovery of the affected limb function was assessed using the MSTS score. The MSTS function score in both groups improved continuously after the operation, but improvement in the 3D-printed group was better than that in the TKR group (Figure 5(a)). The 3D-printed group had a mean score of 23.0 (range, 18–27) at 3 months postoperatively and 28.2 (range, 27–30) at 24 months postoperatively (Figure 6(a)–(d)). The TKR group had a mean score of 20.1 (range, 17–24) at 3 months postoperatively and 26.2 (range, 25–28) at 24 months postoperatively. The differences were statistically significant (3 months postoperatively: T = 2.518, p = 0.019; 12 months postoperatively: T = 4.227, p < 0.001; and 24 months postoperatively: T = 5.433, p < 0.001). The ROM in the 3D-printed group was significantly better than that in the TKR group at 6 and 9 months after the operation (p < 0.05), but no significant difference in ROM was found between the two groups from 1 to 2 years of follow-up (Figure 5(b)).

Table 1. Demographic and oncological data of the patients (n = 26).

Variables	3D-printed group (n = 12)	TKR group (n = 14)	p-value
Demographic data			
Sex			
Male	7 (58.3)	9 (64.3)	0.756
Female	5 (41.7)	5 (35.7)	
Age, years	42.2 ± 11.4	45.4 ± 9.6	0.437
Oncological data			
Site			
Medial femoral condyle	5 (41.7)	6 (42.9)	0.951
Lateral femoral condyle	7 (58.3)	8 (57.1)	
Campanacci classification			0.756
I	0 (0.0)	0 (0.0)	
II	7 (58.3)	9 (64.3)	
III	5 (41.7)	5 (35.7)	

Data are presented as n (%) or mean ± standard deviation.
3D, three-dimensional; TKR, total knee replacement.

Table 2. Statistical comparison of clinical results between the two treatment groups.

Measure	3D-printed group (n = 12)	TKR group (n = 14)	p-value
Operating time, minutes	123.3 ± 20.7	146.4 ± 18.8	0.006
Blood loss, mL	109.6 ± 15.7	182.1 ± 31.9	<0.001
MSTS score after operation			
3 months	23.0 ± 3.1	20.1 ± 2.7	0.019
6 months	24.7 ± 2.1	23.0 ± 1.5	0.020
9 months	26.3 ± 1.5	24.1 ± 1.2	<0.001
12 months	26.7 ± 1.2	24.6 ± 1.3	<0.001
24 months	28.2 ± 0.8	26.2 ± 1.0	<0.001
ROM after operation			
3 months	99.1° ± 7.9°	93.6° ± 9.3°	0.115
6 months	121.7° ± 6.2°	110.7° ± 8.3°	0.001
9 months	124.6° ± 5.0°	118.6° ± 7.2°	0.023
12 months	125.8° ± 4.7°	121.4° ± 7.4°	0.090
24 months	126.3° ± 4.8°	121.8° ± 7.7°	0.097
Local recurrence	0 (0.0)	1 (7.0)	1
Postoperative complications	1 (8.3)	4 (28.6)	0.330

Data are presented as mean ± standard deviation or n (%).
3D, three-dimensional; TKR, total knee replacement; MSTS, Musculoskeletal Tumor Society; ROM, range of motion.

Complications

In the 3D-printed group, one patient had delayed wound healing, and the wound healed after dressing changes without a second operation. No patient developed a deep infection. Postoperative radiographic examinations showed no evidence of bone resorption or osteolysis at the prosthesis–bone interface. No patients developed heterotopic ossification, loosening, breakage, or displacement of the 3D-printed prosthesis.
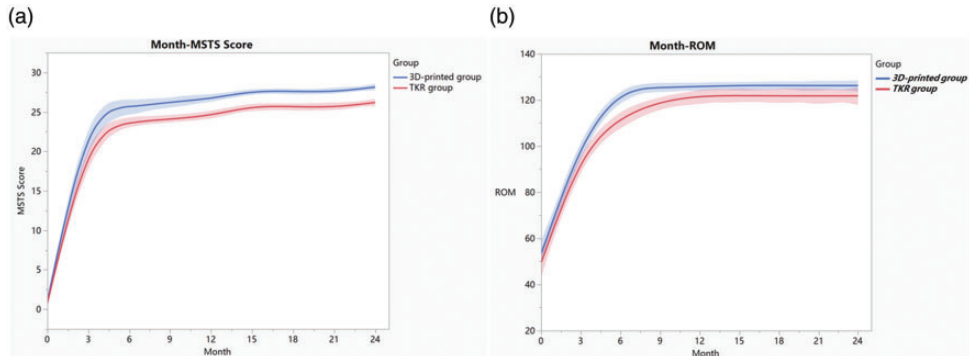
Figure 5. Radiographs taken 26.2 months after 3D-printed prosthesis reconstruction. (a) and (b) No recurrent composite fracture or prosthesis loosening was found.
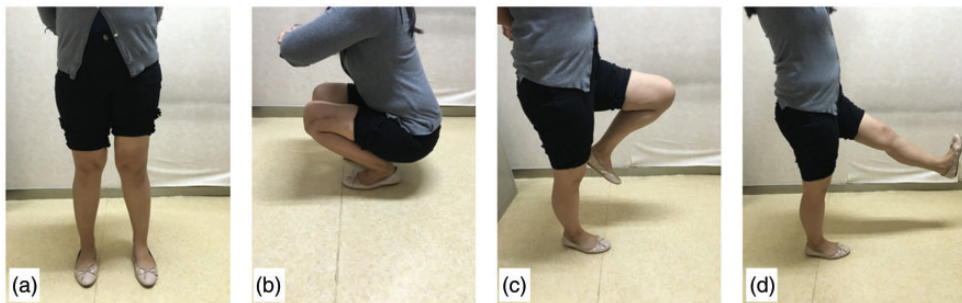

Figure 6. Postoperative recovery of limb function. Satisfactory limb function was present 26.2 months after 3D-printed prosthesis reconstruction. (a) Standing. (b) Crouching. (c) Flexion of the knee. (d) Extension of the knee.

In the TKR group, three patients developed postoperative incision complications (one man and two women), which were related to obesity and a low postoperative albumin concentration. All patients healed 2 weeks after the operation with debridement and catheter flushing. One case of prosthesis loosening occurred 26 months after the operation, and a prosthesis revision was performed.

Discussion

In this study, we used 3D printing technology to help restore a digital model of the anatomic morphology before lesion destruction by using a mirror digital of the

healthy side of the body. The surgical procedures performed in the 3D-printed group had a shorter operating time and less intraoperative blood loss than those performed in the TKR group, and the average values dropped by 15.8% and 39.8%, respectively. These drops in the operating time and bleeding volume indicate that the surgical procedure in the 3D-printed group was less traumatic and complicated. The mean MSTS score in the 3D-printed group was 28.2 (range, 27–30), which was better than that in the TKR group (26.2; range, 25–28) at 24 months postoperatively. The MSTS score in the 3D-printed group was also better than that of patients previously treated with resection, which ranged from

24.5 to 26.0.[16,17] This finding might be associated with less trauma and the use of bone cement, which allows patients to exercise early. We also note that there are many studies to promote local bone healing if bone cement is not used.[18,19] In the 3D-printed group, no composite fracture or prosthesis loosening was found, which is consistent with reports stating that curettage can avoid many complications associated with wide resection.[17,20]

Local control of bone lesions is the primary purpose of surgical treatment.[21–23] The difference between curettage and wide resection is a popular research topic in the treatment of GCTs of bone with pathological fracture.[17,24] Recent studies have shown that curettage can achieve local tumor control rates similar to those of resection while reducing the incidence of complications.[2] Other recent studies have also shown that pathological fractures are not a risk factor for recurrence and that the presence of a pathological fracture should not preclude the decision to perform curettage.[24] A meta-analysis showed a difference in local recurrence rates, but the difference in the risk of local recurrence between the wide resection group and curettage group did not reach statistical significance.[25] Moreover, the meta-analysis suggested that the presence of a pathological fracture should not be the only influencing factor in the decision to perform wide resection or curettage. In our study, all patients in the 3D-printed group underwent curettage before reconstruction of the articular surface, and satisfactory tumor control was achieved during the mean follow-up compared with the TKR group.

If a curettage procedure is chosen in addition to careful intraoperative tumor scraping, then adjuvant therapy is essential[17] to reduce tumor recurrence. After the tumor tissue is scraped off during surgery, local adjuvant therapy (argon beam coagulation, phenol, ethanol, hydrogen peroxide, liquid nitrogen, and others) is often used in the treatment of residual tumor tissue within the lesion.[26] In the 3D-printed group, adjuvant therapy was combined with the use of electric knives, grinding drills, and anhydrous alcohol, and the lesion site was filled with bone cement. Although denosumab has been used in many preoperative studies,[27] we did not use this drug. Some recent literature has suggested that the use of denosumab before curettage may result in a higher recurrence rate because tumor cells are easily retained in the operation.[28,29]

In the 3D-printed group, the joint surface repair material is made of titanium alloy metal. Although an individualized bionic design and high polishing procedure are used, the area of wear of the corresponding tibial articular surface is theoretically larger than the original joint surface, which is believed to accelerate the degeneration of the joint. However, during our follow-up, no significant difference was found in the medial and lateral spaces of the joint in the patients of the 3D-printed group (X-ray film taken while standing). Thus, the wear of the corresponding tibial articular surface may not occur as quickly as previously thought. However, even if surface wear eventually occurs, use of a 3D-printed custom-made prosthesis delays the performance of non-conventional endoprosthesis replacement and reduces the number of revision surgeries. Considering that some postoperative complications of TKA[30,31] and traditional prosthetic revision surgery are often accompanied by lower bone mass and high failure rates,[32] surface repair surgery using 3D-printed custom-made prostheses should benefit patients.

A clear discussion about the limits of application of some surgical treatments is needed. Surface repair surgery using 3D-printed custom-made prostheses is not suitable for all patients with articular surface defects caused by pathological fractures

secondary to GCTs of the distal femur. In our experience, for patients whose joint surfaces of both femoral condyles have articular defects, tumor-type prosthesis replacement is more suitable than surface repair surgery using 3D-printed custom-made prostheses. Patients whose injury involves the cruciate ligament or collateral ligament, especially those with difficult ligament reconstruction, should not undergo surface repair surgery with 3D-printed custom-made prostheses. Tumor-type prosthesis replacement surgery is more suitable for some elderly patients with severe articular surface degeneration rather than the articular surface repair surgery described in this article.

Caution is required in the implementation process of 3D-printed custom-made prostheses in articular surface repair surgery. Implementation should be controlled in all aspects, especially in the following. First, the design of the articular surface and the subsequent high polishing must be precise because these are the keys to reducing joint degeneration. Second, the elastic modulus of the metal articular surface and the normal articular surface are different; thus, the metal articular surface should be 0.5 mm lower than the normal articular surface during design to ensure that the stress of the entire joint is more balanced. Third, the plate added to the articular surface prosthesis should also be designed according to the individualized bone of the patient using 3D printing technology. A well-designed plate can increase the stability of the articular surface prosthesis and provide additional guidance for implantation of the articular surface prosthesis because of its accurate matching with the patient's bone. Finally, the inner side of the articular prosthesis can be designed with protrusions or a porous structure[33] to improve the grip of the bone cement and increase stability.

The main limitation of this study is the relatively short follow-up period.

Loosening and fracture of implants might not occur until several years after the operation. Assessment of the long-term wear of the prosthesis and the corresponding tibial articular surface is required. Survival and oncological outcomes will need to be determined after longer follow-up.

Conclusions

The use of 3D-printed titanium prostheses is growing in musculoskeletal oncology. The use of 3D-printed custom-made prostheses is a promising reconstructive technique for treating unicondylar defects caused by pathological fractures secondary to GCTs of the distal femur. This procedure can achieve satisfactory oncological outcomes and good short-term functional results. Further studies are needed to evaluate the long-term stability of the implants and wear of the articular surface.

Declaration of conflicting interest

The authors declare that there is no conflict of interest.

ORCID iD

Yuqing Ji ⓘD https://orcid.org/0000-0001-6942-6593

References

1. Xu SF, Adams B, Yu XC, et al. Denosumab and giant cell tumour of bone-a review and

future management considerations. *Curr Oncol* 2013; 20: e442–e447.

2. Tsukamoto S, Mavrogenis AF, Tanzi P, et al. Similar local recurrence but better function with curettage versus resection for bone giant cell tumor and pathological fracture at presentation. *J Surg Oncol* 2019; 119: 864–872.

3. Van Der Heijden L, Dijkstra PD, Van De Sande MA, et al. The clinical approach toward giant cell tumor of bone. *Oncologist* 2014; 19: 550–561.

4. Rigollino AV, Fernando TS, Tanaka MH, et al. Giant cell tumor locally advanced around the knee: treatment and literature review. *Rev Bras Ortop* 2017; 52: 473–478.

5. Barut N, Anract P, Babinet A, et al. Periprosthetic fractures around tumor endoprostheses: a retrospective analysis of eighteen cases. *Int Orthop* 2015; 39: 1851–1856.

6. Xu S, Yu X, Xu M, et al. Inactivated autograft-prosthesis composite has a role for grade III giant cell tumor of bone around the knee. *BMC Musculoskelet Disord* 2013; 14: 319.

7. Wang KC, Jones A, Kambhampati S, et al. CT-based 3D printing of the glenoid prior to shoulder arthroplasty: bony morphology and model evaluation. *J Digit Imaging* 2019; 32: 816–826.

8. Park JW, Kang HG, Lim KM, et al. Bone tumor resection guide using three-dimensional printing for limb salvage surgery. *J Surg Oncol* 2018; 118: 898–905.

9. Han Q, Zhao X, Wang C, et al. Individualized reconstruction for severe periprosthetic fractures around the tumor prosthesis of knee under assistance of 3D printing technology: a case report. *Medicine (Baltimore)* 2018; 97: e12726.

10. Wei R, Guo W, Yang R, et al. Reconstruction of the pelvic ring after total en bloc sacrectomy using a 3D-printed sacral endoprosthesis with re-establishment of spinopelvic stability: a retrospective comparative study. *Bone Joint J* 2019; 101-b: 880–888.

11. Angelini A, Trovarelli G, Berizzi A, et al. Three-dimension-printed custom-made prosthetic reconstructions: from revision surgery to oncologic reconstructions. *Int Orthop* 2019; 43: 123–132.

12. Ran Q, Yang W, Hu Y, et al. Osteogenesis of 3D printed porous Ti6Al4V implants with different pore sizes. *J Mech Behav Biomed Mater* 2018; 84: 1–11.

13. Campanacci M, Baldini N, Boriani S, et al. Giant-cell tumor of bone. *J Bone Joint Surg Am* 1987; 69: 106–114.

14. Enneking WF, Dunham W, Gebhardt MC, et al. A system for the functional evaluation of reconstructive procedures after surgical treatment of tumors of the musculoskeletal system. *Clin Orthop Relat Res* 1993: 241–246.

15. Von Elm E, Altman DG, Egger M, et al. The Strengthening the Reporting of Observational Studies in Epidemiology (STROBE) statement: guidelines for reporting observational studies. *Ann Intern Med* 2007; 147: 573–577.

16. Niu X, Zhang Q, Hao L, et al. Giant cell tumor of the extremity: retrospective analysis of 621 Chinese patients from one institution. *J Bone Joint Surg Am* 2012; 94: 461–467.

17. Van Der Heijden L, Dijkstra PD, Campanacci DA, et al. Giant cell tumor with pathologic fracture: should we curette or resect? *Clin Orthop Relat Res* 2013; 471: 820–829.

18. Serbest S, Tiftikçi U, Tosun HB, et al. The irisin hormone profile and expression in human bone tissue in the bone healing process in patients. *Med Sci Monit* 2017; 23: 4278–4283.

19. Serbest S, Tiftikci U, Tosun HB, et al. Is there a relationship between fracture healing and mean platelet volume? *Ther Clin Risk Manag* 2016; 12: 1095–1099.

20. Xing R, Yang J, Kong Q, et al. Giant cell tumour of bone in the appendicular skeleton: an analysis of 276 cases. *Acta Orthop Belg* 2013; 79: 731–737.

21. Çelik S, Uludağ A, Tosun HB, et al. Unicameral (simple) and aneurysmal bone cysts: the effect of insufficient curettage on recurrence. *Pan Afr Med J* 2016; 24: 311.

22. Serbest S, Tiftikçi U, Karaaslan F, et al. A neglected case of giant synovial

chondromatosis in knee joint. *Pan Afr Med J* 2015; 22: 5.

23. Serbest S, Tiftikci U and Uludag A. Unusual localization of a primary hydatid cyst: scaphoid bone: a case report. *Medicine (Baltimore)* 2016; 95: e3290.

24. Salunke AA, Chen Y, Chen X, et al. Does pathological fracture affect the rate of local recurrence in patients with a giant cell tumour of bone?: a meta-analysis. *Bone Joint J* 2015; 97-b: 1566–1571.

25. Salunke AA, Pathak S, Shah J, et al. Wide resection versus curettage in giant cell tumor with pathological fracture? A systematic review and meta-analysis. *J Clin Orthop Trauma* 2018; 9: S15–S18.

26. Greenberg DD and Lee FY. Bisphosphonate-loaded bone cement as a local adjuvant therapy for giant cell tumor of bone: a 1 to 12-year follow-up study. *Am J Clin Oncol* 2019; 42: 231–237.

27. Yang Y, Li Y, Liu W, et al. A nonrandomized controlled study of sacral giant cell tumors with preoperative treatment of denosumab. *Medicine (Baltimore)* 2018; 97: e13139.

28. Errani C, Tsukamoto S, Leone G, et al. Denosumab may increase the risk of local recurrence in patients with giant-cell tumor of bone treated with curettage. *J Bone Joint Surg Am* 2018; 100: 496–504.

29. Scoccianti G, Totti F, Scorianz M, et al. Preoperative denosumab with curettage and cryotherapy in giant cell tumor of bone: is there an increased risk of local recurrence? *Clin Orthop Relat Res* 2018; 476: 1783–1790.

30. Tiftikçi U and Serbest S. Periprosthetic proximal medial femoral cortical destruction caused by a femoral arterial pseudoaneurysm. *Clin Interv Aging* 2015; 10: 1967–1970.

31. Tosun HB, Uludağ A, Serbest S, et al. A rare case of extensive diffuse nonpigmented villonodular synovitis as a cause of total knee arthroplasty failure. *Int J Surg Case Rep* 2014; 5: 419–423.

32. Sevelda F, Waldstein W, Panotopoulos J, et al. Survival, failure modes and function of combined distal femur and proximal tibia reconstruction following tumor resection. *Eur J Surg Oncol* 2017; 43: 416–422.

33. Liang H, Ji T, Zhang Y, et al. Reconstruction with 3D-printed pelvic endoprostheses after resection of a pelvic tumour. *Bone Joint J* 2017; 99-b: 267–275.